Numerical Calculations on Multi-Photon Processes in Alkali Metal Vapors

Nikolaos Merlemis, Andreas Lyras, Georgios Papademetriou, Dionysios Pentaris, and Thomas Efthimiopoulos

Abstract We present the theoretical framework and the approximations needed to numerically simulate the response of alkali metal atoms under multi-photon excitation. By applying the semi-classical approximation, we obtain a system of coupled ordinary and partial differential equations accounting both for the nonlinear dynamics of the atomic medium and the spatiotemporal evolution of the emitted fields. The case of two-photon excitation by a laser field with an additional one-photon coupling field is investigated by numerically solving the set of differential equations employing a self-consistent computational scheme. The computation of the emission intensities and atomic level populations and coherences is then possible.

1 Introduction

Systems of ordinary and partial differential equations have been extensively used in quantum physics and are considered fundamental in order to theoretically understand laser radiation—matter interaction and nonlinear optics. Nonlinear optics is the branch of physics that describes the behavior of light in nonlinear media, that is, media that respond nonlinearly to an applied electromagnetic field

N. Merlemis (✉)
Department of Surveying and Geoinformatics Engineering, University of West Attica, Athens, Greece
e-mail: merlemis@uniwa.gr

A. Lyras
Department of Physics & Astronomy, King Saud University, Riyadh, KSA
e-mail: alyras@ksu.edu.sa

G. Papademetriou · D. Pentaris · T. Efthimiopoulos
Laser Nonlinear and Quantum Optics Labs, Physics Department, University of Patras, Patras, Greece
e-mail: gpapadem@upatras.gr

N. J. Daras, Th. M. Rassias (eds.), *Approximation and Computation in Science and Engineering*, Springer Optimization and Its Applications 180,
https://doi.org/10.1007/978-3-030-84122-5_34

[1]. The nonlinearity is typically observed only at very high light intensities, such as those provided by lasers. In nonlinear optics, the superposition principle no longer holds. Alkali metal atoms have been extensively used as model systems due to their low-lying energy levels. Consequently, the excitation and experimental study of the nonlinear response of alkali metal atom systems using two-photon schemes is easily feasible using laser systems in the visible range of the spectrum. The theoretical description and computation of the nonlinear processes observed in experiments can be implemented using systems of differential equations and by applying either semi-classical approximations, where the atom is treated quantum mechanically but the participating fields classically, or fully quantum descriptions (quantum optics).

Resonant or near resonant multi-photon interaction of laser pulses with atomic systems and the induced nonlinear response in terms of generated radiation have been important research topics. Two-photon excitation, whereby nanosecond (ns) or femtosecond (fs) laser pulses are tuned near a two-photon resonance, has been extensively used to study the atomic system dynamics in a vapor cell. Well known nonlinear phenomena can be easily observed under two-photon excitation, such as the partially coherent amplified spontaneous emission (ASE), stimulated hyper Raman scattering (SHRS) and four-wave mixing emissions (FWM) [2–11]. Forward and backward propagating fields that are emitted axially or conically have also been recorded depending on the laser field detuning and propagation characteristics of the laser beam [12–14]. Excitation of alkali metal vapors have been proven a convenient methodology for the study of phase matching mechanisms, wave mixing emissions, multi-photon mechanisms, energy transfer between atomic states, efficient generation of laser radiation and ultrafast processes [15–27].

Internally generated radiations resulting from the two-photon excitation of alkali metal atoms have been shown to compete with the laser pulse to nonlinearly modify the response of the atomic system, specifically the emitted pulse shapes, the temporal evolution of the emitted pulses and the population distribution in atomic levels. In addition, destructive quantum interference (QI) can take place between laser photons and internally generated photons connecting the same levels modifying the nonlinear response of the system [3, 6, 12, 14, 28]. In addition, several different approaches for the realization of atomic memories in closed systems had been proposed over the past decades [29–32]. Atomic coherence and electromagnetically induced transparency (EIT) [3, 33–37], slow light propagation [38] and lasing without inversion (LWI) [39–43] have been also extensively studied. The theoretical study and experimental demonstration of the manipulation of quantum states between fields and atoms have made feasible the production of quantum memory devices that can efficiently delay or store the quantum states of light fields in order to write, store and "read-out" faithfully these states and the information they carry.

Optical free induction decay (OFID) [44] can become a useful method for studying light-matter interactions, in particular for probing dipole dephasing times in gases and solids. The interaction of an atom with two laser pulses, a pump and a coupling one, in a temporally counterintuitive order (the coupling precedes the pump) have also been considered as an effective method to enhance the nonlin-

earities of an atomic system [45–49]. In general, enhancement of the internally generated fields occurs if the arrival of a pump pulse follows the coherent coupling pulse or if they partially overlap. In the case of a three-level system, the coupling laser, either between the ground and the low excited state (V-type system) or between the two excited states (Λ-type system), creates a coherent superposition of the two states, resulting in enhancement of the parametric emissions driven by the pump laser connecting the ground state to the high excited one [48]. In addition, enhancing the nonlinearities via the use of resonant atomic transitions, has led to the investigation of FWM processes in a counterintuitive pulse sequence [50, 51], which results in the enhancement of the parametric emissions and additional flexibility in their temporal control. It was shown, by using a single pump field, that the response of the system is affected mainly by the pump intensity, the atomic density, and the elastic dephasing collision rates [52]. Finally, observed suppression of emissions due to QI effects, and ionization losses to the continuum (open atomic systems) in the case of focused laser pulses should also be taken into account in computations for a more complete description of the atomic system response [4, 53–60].

In this work, we review the theoretical framework and the approximations needed to simulate the atomic response of alkali metal atoms under two-photon excitation by a laser field. By applying the semi-classical approximation, where the atoms are treated quantum mechanically and the fields classically, we obtain a system of coupled ordinary and partial differential equations for the propagation of the emission fields in the nonlinear atomic medium. The calculation of the emission intensities and the atomic level populations and coherences is then possible after certain additional justifiable approximations are introduced.

2 Theoretical Modeling and Approximations

Two-photon excitation of alkali metal atoms is possible when the orbital angular momentum and parity of the initial $|1\rangle$ and final $|2\rangle$ atomic states satisfy certain selection rules. A typical configuration for the two-photon excitation should include many energy levels having lower energy than $|2\rangle$ (closed system) and possibly the continuum if ionization is taken into account due to absorption of an additional photon (open system). In order to simplify the model and the calculations, the most intense emissions and the associated energy levels are typically included. In this work, the four-level model for the simulation of the atomic system is similar to that presented in [59], where the transition $|1\rangle - |2\rangle$ is excited by two photons, while the de-excitation of atomic state $|2\rangle$ is possible through the lower energy atomic states $|3\rangle$ and $|4\rangle$. The external laser pulse waveform (pump field) used to provide the two photons for the excitation has an intensity which varies with time t. This is simulated in the model either as a secant hyperbolic function $F(t) = \text{sech}^2(t/t_c)$ for $t < 0$ and Gaussian function $F(t) = \exp(-t^2/t_c^2)$ for $t > 0$ or as a single Gaussian function, depending on the waveform characteristics of the experimental laser used to excite the two-photon transition (t_c is the temporal Full Width at Half Maximum

(FWHM) or pulse duration). In order to apply the model and compute the nonlinear response with realistic atomic parameters, potassium atoms are used and levels $|1\rangle$, $|2\rangle$, $|3\rangle$, $|4\rangle$ correspond to the potassium atomic levels $4S_{1/2}$, $6S_{1/2}$, $4P_{3/2}$ and $5P_{3/2}$, respectively. Emissions are generated at one photon allowed transitions (electric dipole selection rules [61]) at frequencies ω_{24}, ω_{41}, ω_{23} and ω_{31} that correspond to the dipole allowed atomic transitions $|2\rangle \leftrightarrow |4\rangle$, $|4\rangle \leftrightarrow |1\rangle$, $|2\rangle \leftrightarrow |3\rangle$ and $|3\rangle \leftrightarrow |1\rangle$.

The semi-classical approximation is used for the interaction of the atom with the electromagnetic field of the laser pulse. This is adequate to simulate experimental results in the case of intense excitation laser fields, where the photon creation and annihilation operators used in a quantum mechanical description of the field can be replaced with the amplitude of the time-dependent classical field. In this case, the Hamiltonian for the interaction of the atom with the electromagnetic field is given by

$$H_I = \frac{1}{2m}[\vec{p} - e\vec{A}(\vec{r}, t)]^2 + e\phi(\vec{r}, t) \tag{1}$$

where $\vec{A}(\vec{r}, t)$ and $\phi(\vec{r}, t)$ are the vector and scalar potentials of the field. In the Coulomb gauge, $\phi(\vec{r}, t) = 0$, and in the dipole approximation, where $\vec{A}(\vec{r}, t) \approx \vec{A}(\vec{r}_0, t)$, we can ignore the spatial derivatives of the vector potential, and using the unitary transformation $|\psi(t)\rangle = \exp\left[\frac{ie\vec{r}}{\hbar} \cdot \vec{A}(\vec{r}, t)\right]|\chi(t)\rangle$ for the state vector and the Schrödinger equation

$$i\hbar\frac{\partial}{\partial t}|\psi(t)\rangle = H|\psi(t)\rangle \tag{2}$$

we can finally write the total Hamiltonian as $H = H_0 + H_I$, where $H_I = -e\vec{r} \cdot \vec{E}(\vec{r}_0, t)$ is the electric dipole interaction Hamiltonian and H_0 the atomic Hamiltonian.

The unitary transformation of the Hamiltonian from the Schrödinger picture to the interaction picture is effected by applying the unitary operator $U_0(t) = \exp[-\frac{i}{\hbar}H_0 t]$:

$$H^{(I)} = U_0^{\dagger} H^{(S)} U_0(t) \tag{3}$$

The free atom Hamiltonian H_0 can be written in the form $H_0 = \sum \hbar\omega_i |i\rangle\langle i|$ where $\hbar\omega_i$ is the energy of the $|i\rangle$ state. Finally, the unitary transformation leads to a Hamiltonian $H^{(I)}$ in the interaction picture [5, 59, 62] that has the form:

$$\begin{aligned} H^{(I)} = &-\hbar(\Omega_{12}^{(2)}|1\rangle\langle 2|e^{-i\Delta_{12}t} + \Omega_{14}|1\rangle\langle 4|e^{-i\Delta_{14}t} + \Omega_{13}|1\rangle\langle 3|e^{-i\Delta_{13}t} + \\ &+ \Omega_{23}|2\rangle\langle 3|e^{-i\Delta_{23}t} + \Omega_{24}|2\rangle\langle 4|e^{-i\Delta_{24}t}) + H.c. \end{aligned} \tag{4}$$

The two-photon Rabi frequency $\Omega_{12}^{(2)}$ is expressed as a linear function of the maximum laser intensity $I_{\max}$ [63]:

$$\Omega_{12}^{(2)}(t) = \frac{\mu_{12}^{(2)}}{c\epsilon_0\hbar} I_{\max} F(t) \tag{5}$$

The two-photon matrix element $\mu_{12}^{(2)}$ is calculated using an effective Green's function approach in the context of the single-channel quantum defect theory [64–67], a technique well established for the calculation of multi-photon matrix elements in alkali metal atoms. The contribution of all non-resonant virtual intermediate states, including the continuum as well, should be included in the calculations. However, taking into account only the contributions of states $|3\rangle$ and $|4\rangle$ is a good approximation in the proposed model. In deriving the density operator equations of motion, the non-resonant virtual atomic levels effectively contributing to the two-photon excitation are adiabatically eliminated. The internally generated radiations, with electric fields

$$E_{ij}(z,t) = \epsilon_{ij}(z,t)\exp[-i(\nu_{ij}t - k_{ij}z)]/2 + c.c. \tag{6}$$

are included in the model in the form of the single-photon Rabi frequencies Ω_{ij}, which are proportional to the complex amplitudes $\epsilon_{ij}(\zeta,t)$ of the emitted fields at transition $|i\rangle \leftrightarrow |j\rangle$. The detuning from the transition $|i\rangle \leftrightarrow |j\rangle$, is denoted as $\Delta_{ij} = \nu_{ij} - \omega_{ij}$, where ν_{ij} is the frequency of the generated field, with indices ij taking values from the set 1, 2, 3, 4 as appropriate. In the computations below, it is assumed that $\Delta_{12} = 0$ (two-photon detuning of the pump) and $\Delta_{ij} = 0$ (single-photon detunings).

In order to derive the equations for the atom, we apply the density operator formulation, where the density operator is defined as $\hat{\rho} = \sum_i a_i |i\rangle\langle i|$ with a_i being the probability of the system to be in the $|i\rangle$ state. Knowing the density operator matrix elements we can extract any information for the atomic system as it can be shown that for an observable A and its corresponding operator $\hat{A}$, the expectation value is $\langle\hat{A}\rangle = \mathrm{Tr}(\hat{\rho}\hat{A})$. The time evolution of the density matrix is governed by the Schrödinger–von Neumann equation: $i\hbar\frac{\partial}{\partial t}\hat{\rho} = [\hat{H},\hat{\rho}]$, where $[\hat{H},\hat{\rho}] = \hat{H}\hat{\rho} - \hat{\rho}\hat{H}$ is the commutator. By applying the rotating wave approximation (RWA) with the transformation $\rho_{ij} = \sigma_{ij}\exp(-i\omega_{ij}t)$, the following set of coupled ordinary differential equations is obtained:

$$\begin{aligned}\dot{\sigma}_{11} = i\big(&\Omega_{12}^{(2)}\sigma_{21} - \Omega_{21}^{(2)}\sigma_{12} + \Omega_{14}\sigma_{41} - \Omega_{41}\sigma_{14} + \\ &+ \Omega_{13}\sigma_{31} - \Omega_{31}\sigma_{13}\big) + \Gamma_{2R}\sigma_{22} + \Gamma_{31}\sigma_{33} + \Gamma_{41}\sigma_{44}\end{aligned} \tag{7}$$

$$\begin{aligned}\dot{\sigma}_{22} = &i(\Omega_{21}^{(2)}\sigma_{12} - \Omega_{12}^{(2)}\sigma_{21} + \Omega_{24}\sigma_{42} - \Omega_{42}\sigma_{24} + \Omega_{23}\sigma_{32} - \Omega_{32}\sigma_{23}) \\ &- (\Gamma_{2R} + \Gamma_{23} + \Gamma_{24})\sigma_{22}\end{aligned} \tag{8}$$

$$\dot{\sigma}_{33} = i(\Omega_{32}\sigma_{23} - \Omega_{23}\sigma_{32} + \Omega_{31}\sigma_{13} - \Omega_{13}\sigma_{31}) - \Gamma_{31}\sigma_{33} + \Gamma_{23}\sigma_{22} \tag{9}$$

$$\dot{\sigma}_{44} = i\big(\Omega_{41}\sigma_{14} - \Omega_{14}\sigma_{41} + \Omega_{42}\sigma_{24} - \Omega_{24}\sigma_{42}\big)$$

$$- \Gamma_{41}\sigma_{44} + \Gamma_{24}\sigma_{22} \tag{10}$$

$$\dot{\sigma}_{12} = i\left(\Delta_{12} + i\left(\gamma_{12} + \gamma_{\text{col}}\right)\right)\sigma_{12} + i\Omega_{12}^{(2)}(\sigma_{22} - \sigma_{11}) + \\ + i\left(\Omega_{14}\sigma_{42} + \Omega_{13}\sigma_{32} - \Omega_{32}\sigma_{13} - \Omega_{42}\sigma_{14}\right) \tag{11}$$

$$\dot{\sigma}_{13} = i\left(\Delta_{13} + i(\gamma_{13} + \gamma_{\text{col}})\right)\sigma_{13} + i\Omega_{13}(\sigma_{33} - \sigma_{11}) \\ + i\left(\Omega_{41}\sigma_{43} + \Omega_{12}\sigma_{23} - \Omega_{23}\sigma_{12}\right) \tag{12}$$

$$\dot{\sigma}_{14} = i\left(\Delta_{14} + i\left(\gamma_{14} + \gamma_{\text{col}}\right)\right)\sigma_{14} + i\Omega_{14}(\sigma_{44} - \sigma_{11}) + \\ + i(\Omega_{12}^{(2)}\sigma_{24} + \Omega_{13}\sigma_{34} - \Omega_{24}\sigma_{12}) \tag{13}$$

$$\dot{\sigma}_{23} = -i\left(\Delta_{12} - \Delta_{13} - i\left(\gamma_{23} + \gamma_{\text{col}}\right)\right)\sigma_{23} + i\left(\Omega_{23}(\sigma_{33} - \sigma_{22}) + \\ + \Omega_{21}^{(2)}\sigma_{13} + \Omega_{24}\sigma_{43} - \Omega_{13}\sigma_{21}\right) \tag{14}$$

$$\dot{\sigma}_{24} = -i\left(\Delta_{12} - \Delta_{14} - i\left(\gamma_{24} + \gamma_{\text{col}}\right)\right)\sigma_{24} + \\ + i\left(\Omega_{24}(\sigma_{44} - \sigma_{22}) + \Omega_{21}^{(2)}\sigma_{14} + \Omega_{23}\sigma_{34} - \Omega_{14}\sigma_{21}\right) \tag{15}$$

$$\dot{\sigma}_{34} = -i\left(\Delta_{14} - \Delta_{13} - i\left(\gamma_{34} + \gamma_{\text{col}}\right)\right)\sigma_{34} + i\left(\Omega_{31}\sigma_{14} + \Omega_{32}\sigma_{24} - \right. \\ \left. - \Omega_{14}\sigma_{31} - \Omega_{24}\sigma_{32}\right) \\ + \text{c. c.} \tag{16}$$

The coherence decay rates of the four-level model system of potassium atom are phenomenologically added as γ_{12}, γ_{24}, γ_{41}, γ_{23}, γ_{31} and they are calculated by the formula $\gamma_{ij} = \sum \Gamma_{ij}/2$, $(i \neq j)$, where the decay constant Γ_{ij} is the inverse lifetime (ns^{-1}) of transition $|i\rangle \leftrightarrow |j\rangle$ [5, 62, 68–71]. In addition, the contribution of collision dephasing rate γ_{col} is considered in the non-diagonal density matrix elements, simulating the elastic collisions of potassium atom with the buffer gas used in the experiments. The effective decay Γ_{2R} in (7), is obtained from the contribution of the states $|4\rangle$, $|3\rangle$ and the intermediate ones $|3D_{3/2}\rangle$ and $|5S_{1/2}\rangle$, through which the atom decays from the state $|2\rangle$ to $|1\rangle$ [3, 5, 31].

In order to account for the generation of the internally generated fields and their propagation along the z axis, the Maxwell equations are used for the field amplitudes (or Rabi frequencies) within the slowly varying envelope approximation (SVEA). Transformed in the retarded time frame by the transformation $\tau = t - z/c$ and $z = \zeta$, they read as:

$$\frac{\partial}{\partial \zeta}\Omega_{ij}(\zeta, \tau) = i\frac{k_{ij}}{4\epsilon_0\hbar}\mu_{ij}\, p_{ij}(\zeta, \tau)$$

where $p_{ij}(\zeta, \tau) = N\text{Tr}(\hat{\mu}\hat{\rho})$ is the quantum mechanical atomic polarization, N the atomic density of potassium, ϵ_0 the permittivity of free space, k_{ij} the wave-number for each transition and μ_{ij} the matrix element of the electric dipole operator for the

corresponding single-photon transition [63]. The matrix elements of the transitions of interest are taken from [61]: $\mu_{24} = 10.7$ a.u., $\mu_{41} = -0.453$ a.u., $\mu_{23} = 1.07$ a.u. and $\mu_{31} = -5.13$ a.u., respectively. The two-photon matrix element of the pumping transition is calculated to be $\mu_{12}^{(2)} = -950$ a.u., where a.u. denotes atomic units [63]. Finally, the propagation equations for the internally generated Rabi frequencies in a co-propagating reference frame assumed the following form:

$$\frac{\partial}{\partial \zeta}\Omega_{24}(\zeta,\tau) = iN\,\frac{k_{24}}{2\epsilon_0\hbar}\,\mu_{24}^2\sigma_{24} \tag{17}$$

$$\frac{\partial}{\partial \zeta}\Omega_{41}(\zeta,\tau) = iN\,\frac{k_{41}}{2\epsilon_0\hbar}\,\mu_{14}^2\sigma_{41} \tag{18}$$

$$\frac{\partial}{\partial \zeta}\Omega_{23}(\zeta,\tau) = iN\,\frac{k_{23}}{2\epsilon_0\hbar}\,\mu_{23}^2\sigma_{23} \tag{19}$$

$$\frac{\partial}{\partial \zeta}\Omega_{31}(\zeta,\tau) = iN\,\frac{k_{31}}{2\epsilon_0\hbar}\,\mu_{13}^2\sigma_{31} \tag{20}$$

The set of coupled equations (7)–(20) are the Maxwell-Bloch equations of our system and can be numerically solved self-consistently obtaining the spatiotemporal dependence for the unknown quantities Ω_{ij} and σ_{ij}. The intensity I_{ij} of the generated emissions is calculated as $I_{ij} = \frac{2\hbar^2\epsilon_0 c}{\mu_{ij}^2}\Omega_{ij}^2$.

In addition, transition $|4\rangle \leftrightarrow |1\rangle$ or $|3\rangle \leftrightarrow |1\rangle$ can be excited in our model by an external field in order to compute the characteristics of the system under a V-type coupling scheme (laser pump field excites the two-photon transition while an external coupling field is applied on the one-photon transition). The tunable external coupling field is considered to have maximum intensity I_{14}^c and the same waveform and duration as the pump laser field, in a pump-coupling excitation scheme. In the case of $|4\rangle \leftrightarrow |1\rangle$ coupling (V_{14} coupling scheme), the new coupling Rabi frequency denoted as $\Omega_{14}^c = \frac{\mu_{14}}{2\hbar}\sqrt{\frac{2}{c\epsilon_0}}\sqrt{|I_{14}^c|}F(\tau)$ is added in every term containing Ω_{14} replacing Ω_{14} with $(\Omega_{14}+\Omega_{14}^c)$ and Ω_{41} with $(\Omega_{41}+\Omega_{14}^c)$ in the set of Eqs. (7), (10), (11), (12), (13), (15), and (16), while the system interaction Hamiltonian describing the V-type coupling scheme takes the following form:

$$\begin{aligned} H^{(I)} = &-\hbar(\Omega_{12}^{(2)}|1\rangle\langle 2|e^{-i\Delta_{12}t} + (\Omega_{14}+\Omega_{14}^c)|1\rangle\langle 4|e^{-i\Delta_{14}t} + \Omega_{13}|1\rangle\langle 3|e^{-i\Delta_{13}t} + \\ &+ \Omega_{23}|2\rangle\langle 3|e^{-i\Delta_{23}t} + \Omega_{24}|2\rangle\langle 4|e^{-i\Delta_{24}t}) + H.c. \end{aligned} \tag{21}$$

We assume that both external fields resonantly excite the transitions of interest and as a consequence $\Delta_{12} = 0$ and $\Delta_{14}^c = 0$ (the latter is the coupling field detuning). The $|3\rangle \leftrightarrow |1\rangle$ external excitation (V_{13} coupling scheme) can be investigated in a similar way.

Furthermore, an external coupling laser field with maximum intensity I_{23}^c and the same waveform and duration can be used to excite the upper single-photon

transition $|2\rangle \leftrightarrow |3\rangle$, in a Λ-type pump-coupling scheme. In this case, the Rabi frequency of the coupling field is defined as $\Omega_{23}^{c} = \frac{\mu_{23}}{2\hbar}\sqrt{\frac{2}{c\epsilon_0}}\sqrt{|I_{23}^{c}|}F(\tau)$, and both pump and coupling fields are assumed to resonantly excite the transitions of interest, so $\Delta_{12} = 0$ and $\Delta_{23}^{c} = 0$ (single-photon detuning of the coupling). The coupling Rabi frequency is also added in every term containing Ω_{23} and Ω_{32} in the set of Eqs. (8), (9), (11), (12), (14), (15) and (16) with the new Hamiltonian describing the Λ-type coupling scheme being:

$$H^{(I)} = -\hbar(\Omega_{12}^{(2)}|1\rangle\langle 2|e^{-i\Delta_{12}t} + \Omega_{14}|1\rangle\langle 4|e^{-i\Delta_{14}t} + \Omega_{13}|1\rangle\langle 3|e^{-i\Delta_{13}t} + \\ + (\Omega_{23} + \Omega_{23}^{c})|2\rangle\langle 3|e^{-i\Delta_{23}t} + \Omega_{24}|2\rangle\langle 4|e^{-i\Delta_{24}t}) + H.c. \tag{22}$$

The enhancements observed for the internally generated emissions in the case of a V-type or a Λ-type coupling scheme are discussed in [69–71].

An important phenomenon that can interfere with the model described is the ionization process. In the previous discussion, the atomic system is presented as a closed system, meaning that the atoms are excited and participate in several processes due to the interaction with the electromagnetic fields, but they remain unaltered (no electrons are absorbed or lost) and finally, after a certain period of time, the atoms return to their original state $|1\rangle$. This means that the number of participating atoms in the model remains constant. However, ionization processes are possible due to the strong intensities of the electromagnetic fields used, for example, three pump laser photons can cause the extraction of an electron and the subsequent ionization of the atom. Since ionized atoms are different than the neutral atoms and the model becomes extremely complicated if ions are also taken into account, a different approach is needed. In order to take into consideration the ionization process, we assume that ions generated are extracted from the system and do not participate in the model. Consequently, we discuss the atomic model as an open system in which neutral atoms population decreases with time. The effect of the ionization process (transition to the continuum) was presented in [59] in the case of the potassium atom.

In order to include the transition to the continuum through the two-photon resonant, three-photon ionization mechanism [62], the Maxwell-Bloch equations have to be transformed. At first, the sum of the population derivatives is non-zero, in contrast to a closed four-level system, so Eq. (8) has to be modified by the addition of the term $-\Gamma_{ion} I_{max} F(\tau)\sigma_{22}$.

I_{max} is the pump laser peak intensity and Γ_{ion} is the ionization width (more information about the ionization rate in an open atomic system can be found in [59]). In addition, the term $-\Gamma_{ion} I_{max} F(\tau)\sigma_{mn}/2$ must be added in Eqs. (11), (14), and (15), since all transitions connected with state $|2\rangle$ are affected by the transition from the state to the continuum (quantified by the factor Γ_{ion}) due to the two-photon resonant, three-photon ionization process. Furthermore, in order to take into account ionization from state $|4\rangle$ (system loses from state $|4\rangle$ to the continuum) by the absorption of one laser photon, the term $-\Gamma'_{ion} I_{max} F(\tau)\sigma_{44}$ is also added in

Eq. (10), and the term $-\Gamma'_{ion} I_{max} F(\tau)\sigma_{mn}/2$ is also added in Eqs. (13), (15), and (16), which are related to the off-diagonal matrix elements.

For short laser pulses, such as in the femtosecond (fs) range, the propagation of both the pump and coupling laser fields in the medium has to be taken into account. For the coupling Rabi frequency we add another equation in the form of (17)–(20):

$$\frac{\partial}{\partial\zeta}\Omega_c(\zeta,\tau) = iN\frac{k_c}{2\epsilon_0\hbar}\mu_c^2\sigma_c \tag{23}$$

where c is to be replaced with the appropriate numbers of the coupled transitions. The two-photon field propagation is governed [12] by the equation

$$\frac{\partial}{\partial\zeta}\Omega_{12}^{(2)}(\zeta,\tau) = iN\frac{k_{12}}{2\epsilon_0\hbar}4K_{12}^{(2)}\sigma_{12}\Omega_{12}^{(2)} \tag{24}$$

where the second order coupling strength $K_{12}^{(2)} = \frac{1}{2\hbar}\sum_i \frac{\mu_{2i}\mu_{i1}}{\omega_{2i}-\omega_1}$ is calculated over all the virtual states between the states $|1\rangle$ and $|2\rangle$.

3 Results and Discussion

The set of differential equations (7)–(20) and (23), (24) is numerically solved employing a FORTRAN code. We calculate both the field and atomic variables by taking alternate steps in space and time along two grids of constant step size, one spatial, along the propagation axis, and one temporal, starting from known initial conditions for the atomic variables at each position and known boundary conditions for the field variables at each time [72]. Initially, the atoms are considered to be at the ground state for each ζ at $\tau = 0$, while the boundary conditions for the generated Rabi frequency Ω_{ij} at $\zeta_0 = 0$ correspond to the quantum noise level, which induces single-photon transitions by quantum fluctuations, with a typical value of $\Omega_{ij}(0,\tau) \propto \epsilon_0(0,\tau) = 10^{-4}$ V/cm [73].

To solve the first-order coupled differential equations, either with respect to time or with respect to position, we employ the fourth-order Runge–Kutta method of constant step size. This method is simple but sufficiently accurate and allows for explicit control of the step sizes to match the requirements of the physics problem and provide the necessary detail in the representation of the evolution of both the atomic and field variables. In our system both the duration of the pump pulse and the total propagation length are fixed. We have chosen to advance the set of variables in time at discrete positions and we typically study the outcome at the exit face of the vapor cell that allows us to compare directly with experimental results.

However, for short, sub-ps pulsed excitation a very small time step is needed to accurately describe the atomic and field evolution, even more so since the pump pulse should be also propagated. In typical computing platforms, the execution time of the code becomes prohibitively large, so the total propagation length was limited

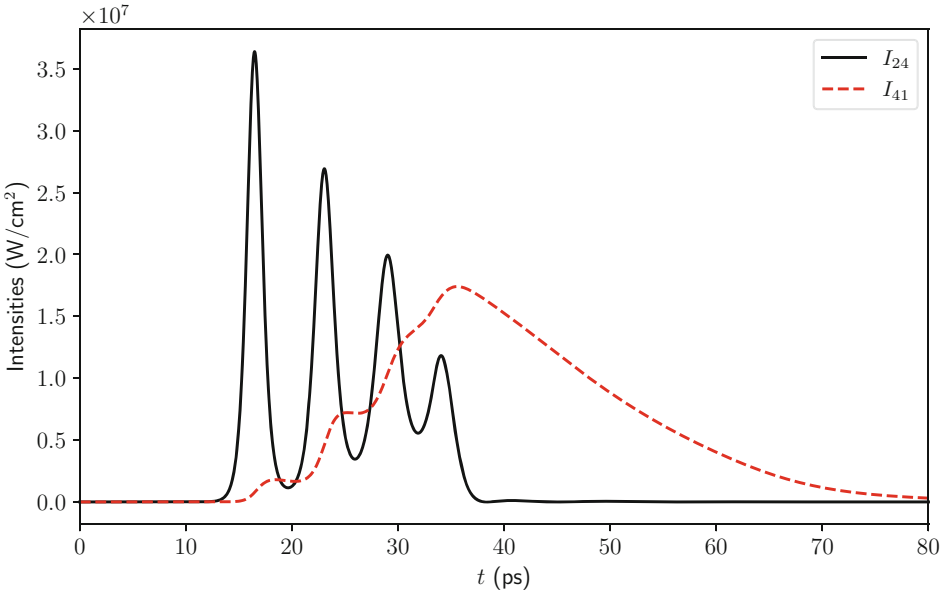

Fig. 1 Intensities versus time for the internally generated emissions at the $|2\rangle - |4\rangle$ and the $|4\rangle - |1\rangle$ transitions. The system parameters are: Laser intensity $I_{\max} = 45\,\mathrm{GW/cm^2}$, coupling intensity $I_{14}^{c} = 5\,\mathrm{W/cm^2}$, pulses FWHM $\tau_c = 40\,\mathrm{fs}$, pump-coupling temporal separation $\Delta t = -2\,\mathrm{ps}$ and atomic density $N = 4 \times 10^{15}\,\mathrm{cm^{-3}}$

to 1 cm. This length corresponds to typical vapor cell sizes used in experimental setups and, in principle, longer propagation lengths can be studied numerically given sufficient computational resources.

In the following computations the atomic system is assumed to be open in order to take into account ionization processes. Short pulse excitation (0.04 ps pulses) and a V-coupling scheme are applied, with the coupling field having the same pulse characteristics as the excitation pulse applied at the two-photon transition. In this case, emissions at ω_{24} and ω_{41} partially overlap temporally within the excitation pulse duration and are clearly synchronized as is evident in Fig. 1. Populations of state $|3\rangle$ and emissions at ω_{23} and ω_{31} remain in the noise regime for the parameters used in our model, so they are not shown in the following figures and discussion.

In Fig. 2, the populations of the atomic states are shown. It is evident that state $|3\rangle$ remains unpopulated at all times and that state $|2\rangle$ builds its maximum population during the short excitation pulse duration of 0.04 ps. The system assumes a steady state driven by short pulses of internally generated emissions and subsequently spontaneous decay that drives the population back to the ground state via a cascade of emissions. The time scale of spontaneous emission is far longer than the one depicted in the figures.

Further insight into the evolution of the internally generated emissions is provided by the study of the coherences, i.e., the off-diagonal matrix elements of the atomic density operator. In Fig. 3a and b the calculated time profiles of both σ_{24} and σ_{41} are depicted. Their time evolution correlates well with the calculated intensities for the corresponding emissions, shown in Fig. 1. In particular, the time

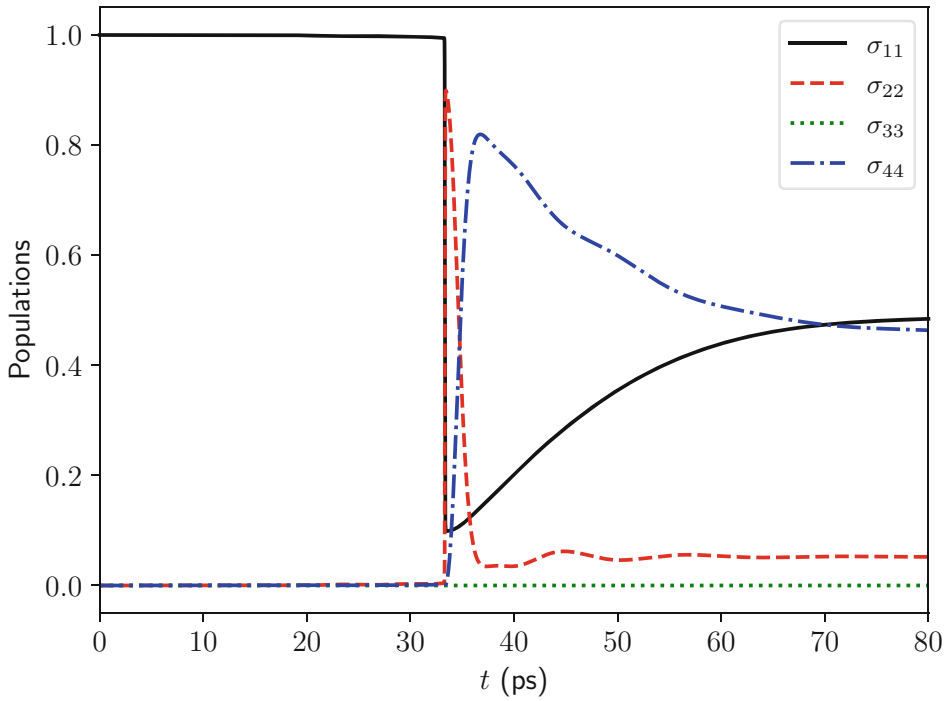

Fig. 2 Populations of the states $|1\rangle \leftrightarrow |4\rangle$ versus time. The system parameters are the same as in Fig. 1

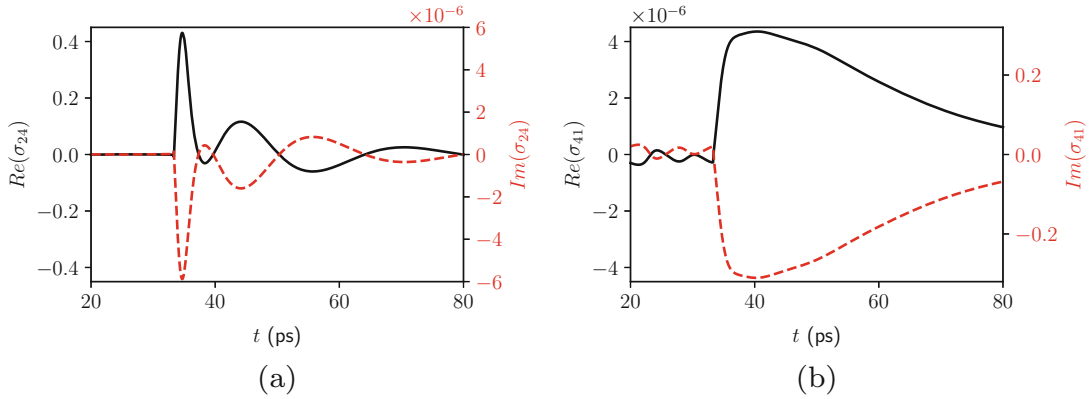

Fig. 3 Coherences of the $|2\rangle \leftrightarrow |4\rangle$ (**a**) and of the $|4\rangle \leftrightarrow |1\rangle$ (**b**) transition versus time. The system parameters are the same as in Fig. 1

evolution of the imaginary parts of both coherences provides an insight into the multi-peaked emission profile at ω_{24} and the gradual build-up and broad emission profile at ω_{41}.

The introduction of a weak coupling pulse, either in the $|1\rangle \leftrightarrow |3\rangle$ or the $|2\rangle \leftrightarrow |3\rangle$ transitions, transforms the system's dynamics, and significantly enhances the ω_{23} and ω_{31} radiations, while no significant population in state $|3\rangle$ is obtained. In Fig. 4 the coupling field connecting the $|1\rangle \leftrightarrow |3\rangle$ states (V_{13} coupling scheme) with maximum intensity $I_{13}^{c} = 1\,\mathrm{kW/cm^2}$ enhance the emissions via state $|3\rangle$ (termed path-2 emissions) several orders of magnitude, while the emissions via state $|4\rangle$

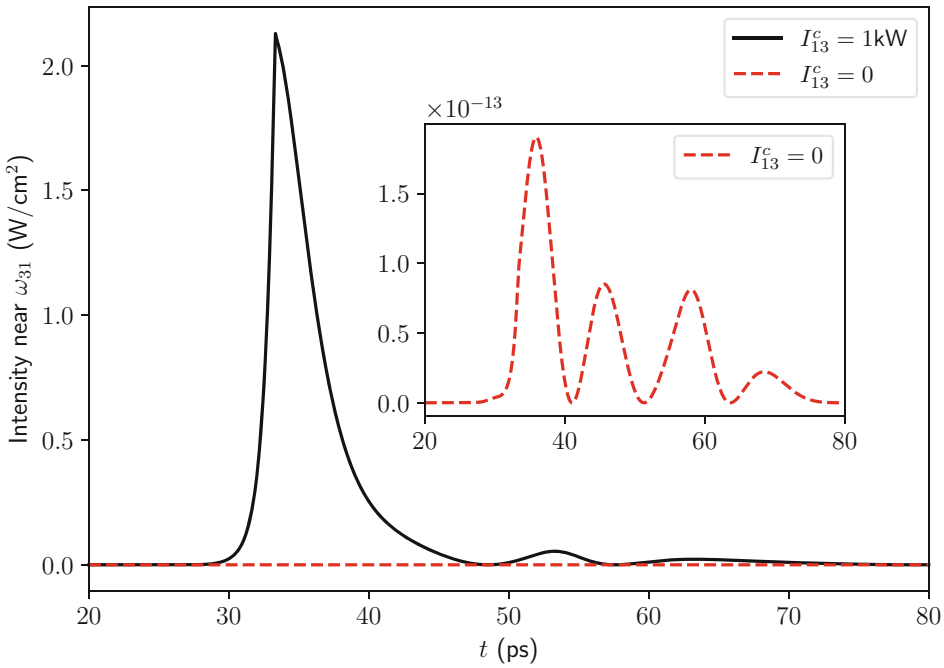

Fig. 4 Intensities of the ω_{31} emission with excitation intensity 45GW/cm^2 and a $|1\rangle$-$|3\rangle$ coupling field of $I_{13}^c = 1$kW/cm^2 (solid line) and without the coupling field (dashed line). The enhancement of the ω_{31} emission is 13 orders of magnitude

(termed path-1 emissions) are unaffected. Furthermore, the internally generated path-2 radiations are synchronous to the path-1 ones and to the excitation pulse, an indication of a parametric process. For a coupling pulse of strength comparable to the excitation pulse, the dynamics of the system is reversed and the energy is transferred through the path-2 emissions while the path-1 ones are negligible. The reliable numerical investigation of the system dynamics offers valuable insights for the efficient control of the emissions in the system, guiding future experimental work.

The relative temporal delay of the two pulses can be used to estimate the coherence relaxation time (CRT) of the atomic states. For the V_{14} or the V_{13} coupling schemes, the induced coherence by the coupling field, when it precedes the pump, enhances the ω_{41} or the ω_{31} emissions, so the exponential increase in the corresponding intensities, that can be accurately calculated as a function of time, can provide an estimate the CRT of the $|4\rangle$ or the $|3\rangle$ states, respectively. When the coupling pulse follows the pump, the effect on the ω_{41} or ω_{31} emissions is governed by the σ_{12} coherence and the calculated exponential decrease in the corresponding intensities provides an estimate of the CRT of the $|2\rangle$ state. The theoretical calculations are in good agreement with the experiment [70, 71] in the V_{14} system. The coupling field in a Λ configuration which connects the upper $|2\rangle$ state with the $|4\rangle$ or the $|3\rangle$ ones, does not induce coherence when it precedes the pump (negative temporal delay), a condition that was observed both in the experiment and in the theoretical calculations [62], where it is shown that for

positive temporal delays the ω_{41} or ω_{31} radiation enhancement can provide an estimate of the CRT for the $|2\rangle$ state.

4 Conclusions

The semi-classical approximation, where the atoms are treated quantum mechanically and the fields classically, is employed in order to compute the atomic response of alkali metal atoms under different multi-photon processes. In the case of a four-level atomic system and two-photon excitation by a laser field, a system of coupled linear ordinary and partial differential equations is numerically solved self-consistently in order to compute the atomic parameters (populations and coherences) and the emission fields propagating in the nonlinear atomic medium. The numerical solution provides a comprehensive spatiotemporal description of the evolution of both the driven atomic system and the input and internally generated fields that afford direct comparison with experimental results.

References

1. R. Boyd, *Nonlinear Optics*, 3rd edn. (Academic Press, London, 2008)
2. M. Katharakis, N. Merlemis, A. Serafetinides, T. Efthimiopoulos, Four-wave mixing and parametric four-wave mixing near the 4P-4S transition of the potassium atom. J. Phys. B-Atomic Mol. Optical Phys. **35**(24), 4969–4980 (2002)
3. N. Merlemis, M. Katharakis, E. Koudoumas, T. Efthimiopoulos, Stimulated emissions and quantum interference in potassium atom-laser interaction. J. Phys. B-Atomic Mol. Optical Phys. **36**(10), 1943–1956 (2003)
4. L. Deng, M.G. Payne, W.R. Garrett, Effects of multi-photon interferences from internally generated fields in strongly resonant systems. Phys. Rep. **429**(3–4), 123–241 (2006)
5. A. Armyras, D. Pentaris, T. Efthimiopoulos, N. Merlemis, A. Lyras, Saturation and population transfer of a two-photon excited four-level potassium atom. J. Phys. B: At. Mol. Opt. Phys. **44**(16), 165401 (2011)
6. G. Morigi, S. Franke-Arnold, G. L. Oppo, Phase-dependent interaction in a four-level atomic configuration. Phys. Rev. A At. Mol. Opt. Phys. **66**(5), 9 (2002)
7. E.A. Korsunsky, T. Halfmann, J.P. Marangos, K. Bergmann, Analytical study of four-wave mixing with large atomic coherence. Eur. Phys. J. D **23**(1), 167–180 (2003)
8. S. Kajari-Schröder, G. Morigi, S. Franke-Arnold, G.-L. Oppo, Phase-dependent light propagation in atomic vapors. Phys. Rev. A **75**(012816), 1–14 (2007)
9. D. Pentaris, T. Efthimiopoulos, N. Merlemis, V. Vaičaitis, Axial and conical parametric emissions from potassium atoms under two-photon fs excitation. Appl. Phys. B: Lasers Opt. **98**(2–3), 383–390 (2010)
10. V. Vaičaitis, V. Jarutis, D. Pentaris, Conical third-harmonic generation in normally dispersive media. Phys. Rev. Lett. **103**(10), 4–7 (2009)
11. I. Pop, L. Moorman, Electromagnetically induced generation, gain in delayed wave mixing, and measuring coherent states using quantum-interference windows. Phys. Rev. A **60**(1), 678–686 (1999)

12. T. Efthimiopoulos, N. Merlemis, M. E. Movsessian, D. Pentaris, M. Katharakis, Action of counter-propagating laser beams on two-photon excitation of potassium vapour. J. Phys. B: At. Mol. Opt. Phys. **43**(5), 055401 (2010)
13. H. Skenderović, T. Ban, N. Vujičić, D. Aumiler, S. Vdović, G. Pichler, Cone emission induced by femtosecond excitation in rubidium vapor. Phys. Rev. A **77**(063816), 1–6 (2008)
14. R.K. Wunderlich, W.R. Garrett, R.C. Hart, M.A. Moore, M.G. Payne, Nonlinear optical processes near the sodium 4 D two-photon resonance. Phys. Rev. A **41**(11), 6345–6360 (1990)
15. H. Yu, F. Chen, Y. He, Q. Pan, D. Yu, J. Xie, Nonlinear phase matching in parametric four-wave mixing process of Cs vapor. Optik **205**, 163583 (2020)
16. M. M. Curčić, T. Khalifa, B. Zlatković, I.S. Radojičić, A.J. Krmpot, D. Arsenović, B.M. Jelenković, M. Gharavipour, Four-wave mixing in potassium vapor with an off-resonant double-Λ system. Phys. Rev. A **97**(6), 063851 (2018)
17. Z. Chang-Jun, H. Jun-Fang, X. Bing, Z. Xue-Jun, Observation of quantum beat in Rb by parametric four-wave mixing. Chin. Phys. Lett. **24**(8), 2234–2237 (2007)
18. G. Shi, C. Zhu, B. Xue, X. Zhai, Control of two IR signals from coupled parametric six-wave mixing processes in Rb vapor. Optik **126**(20), 2278–2281 (2015)
19. B. Zlatković, A.J. Krmpot, N. Šibalić, M. Radonjić, B.M. Jelenković, Efficient parametric non-degenerate four-wave mixing in hot potassium vapor. Laser Phys. Lett. **13**(1), 015205 (2016)
20. H. Yu, F. Chen, Q. Pan, Y. He, J. Xie, Modeling and analysis of the pumping threshold characteristics in one-color two-photon excited Cs vapor. IEEE J. Quantum Electron. **56**(2), 1500106 (2020)
21. N.R. De Melo, S.S. Vianna, Frequency shift in three-photon resonant four-wave mixing by internal atom-field interaction. Phys. Rev. A: At. Mol. Opt. Phys. **92**(5), 053830 (2015)
22. M. Głódź, A. Huzandrov, S. Magnier, L. Petrov, I. Sydoryk, J. Szonert, J. Klavins, K. Kowalski, Energy transfer reaction K(4s) + K(7s)→ K(4s) + K(5f), theory compared with experiment. J. Quant. Spectrosc. Radiat. Transf. **227**, 152–169 (2019)
23. B.V. Zhdanov, R.J. Knize, DPAL: historical perspective and summary of achievements, in *Technologies for Optical Countermeasures X; and High-Power Lasers 2013: Technology and Systems*, ed. by D.H. Titterton, M.A. Richardson, R.J. Grasso, H. Ackermann, W.L. Bohn, vol. 8898 (SPIE, 2013), p. 88980V
24. B.V. Zhdanov, R.J. Knize, Advanced diode-pumped alkali lasers, in *Advanced Laser Technologies 2007*, ed. by I.A. Shcherbakov, R. Myllylä, A.V. Priezzhev, M. Kinnunen, V.I. Pustovoy, M.Y. Kirillin, A.P. Popov, vol. 7022 (SPIE, 2008), p. 70220J
25. B.V. Zhdanov, R.J. Knize, Diode pumped alkali lasers, in *Technologies for Optical Countermeasures VIII*, ed. by D.H. Titterton, M.A. Richardson, vol. 8187 (SPIE, 2011), p. 818707
26. Y. Makdisi, J. Kokaj, K. Afrousheh, R. Nair, J. Mathew, G Pichler, Femtosecond laser fluorescence and propagation in very dense potassium vapor. Opt. Exp. **21**(25), 30306 (2013)
27. Z.H. Lu, C.J. Zhu, A.A. Senin, J.R. Allen, J. Gao, J.G. Eden, Production and probing of atomic wavepackets with ultrafast laser pulses: Applications to atomic and molecular dynamics. IEEE J. Sel. Topics Quantum Electron. **10**(1), 159–168 (2004)
28. W.R. Garrett, M.A. Moore, R.C. Hart, M.G. Payne, R. Wunderlich, Suppression effects in stimulated hyper-Raman emissions and parametric four-wave mixing in sodium vapor. Phys. Rev. A **45**(9), 6687–6709 (1992)
29. C. Liu, Z. Dutton, C.H. Behroozi, L. Vestergaard Hau, L.V. Hau, Observation of coherent optical information storage in an atomic medium using halted laser pulses. Nature **409**(6819), 490–493 (2001)
30. Y.O. Dudin, L. Li, A. Kuzmich, Light storage on the time scale of a minute. Phys. Rev. A: At. Mol. Opt. Phys. **87**(3), 1–4 (2013)
31. D. Pentaris, T. Marinos, N. Merlemis, T. Efthimiopoulos, Optical free induction memory in potassium vapor under a partially-truncated two-photon excitation. J. Mod. Opt. **56**(6), 840–850 (2009)
32. O. Katz, O. Firstenberg, Light storage for one second in room-temperature alkali vapor. Nat. Commun. **9**(1), 2074 (2018)

33. S.E. Harris, R.B. Miles, Proposed third-harmonic generation in phase-matched metal vapors. Appl. Phys. Lett. **19**(10), 385–387 (1971)
34. S.E. Harris, Electromagnetically induced transparency. Phys. Today **50**(7), 36–42 (1997)
35. D.A. Braje, V. Balić, S. Goda, G.Y. Yin, S.E. Harris, Frequency mixing using electromagnetically induced transparency in cold atoms. Phys. Rev. Lett. **93**(18), 18–21 (2004)
36. E. Paspalakis, N.J. Kylstra, P.L. Knight, Transparency induced via decay interference. Phys. Rev. Lett. **82**(10), 2079–2082 (1999)
37. M.D. Eisaman, A. André, F. Massou, M. Fleischhauer, A.S. Zibrov, M.D. Lukin, Electromagnetically induced transparency with tunable single-photon pulses. Nature **438**(7069), 837–841 (2005)
38. E. Paspalakis, P.L. Knight, Transparency, slow light and enhanced nonlinear optics in a four-level scheme. J. Opt. B: Quantum Semiclassical Opt. **4**(4), 372–375 (2002)
39. J. Mompart, R. Corbalan, Lasing without inversion. J. Opt. B **2**, 7–24 (2000)
40. N. Merlemis, A. Lyras, M. Katharakis, T. Efthimiopoulos, Amplified spontaneous emission without population inversion in potassium vapour by internally generated fields. J. Phys. B: At. Mol. Opt. Phys. **39**(8), 1913–1927 (2006)
41. S.E. Harris, Lasers without inversion: interference of lifetime-broadened resonances. Phys. Rev. Lett. **62**(9), 1033–1036 (1989)
42. D. Braunstein, R. Shuker, Dressed states analysis of lasing without population inversion in a three-level ladder scheme: approximate analytic time dependent solutions. Laser Phys. **19**(2), 290–304 (2009)
43. J.-C. Liu, Y.-Q. Zhang, L. Chen, Coherent control of nondegenerate two-photon absorption by femtosecond laser pulses. J. Mod. Opt. **61**(10), 781–786 (2014)
44. R.G. Brewer, R.L. Shoemaker, Optical free induction decay. Phys. Rev. A **6**(6), 2001–2007 (1972)
45. K. Boller, A. Imamolu, S.E. Harris, Observation of electromagnetically induced transparency. Phys. Rev. Lett. **66**(20), 2593–2596 (1991)
46. J.E. Field, K.H. Hahn, S.E. Harris, Observation of electromagnetically induced transparency in collisionally broadened lead vapor. Phys. Rev. Lett. **67**(22), 3062–3065 (1991)
47. K. Hakuta, L. Marmet, B.P. Stoicheff, Nonlinear optical-generation with reduced absorption using electric-field coupling in atomic-hydrogen. Phys. Rev. A **45**(7), 5152–5159 (1992)
48. R.I. Thompson, B.P. Stoicheff, G.Z. Zhang, K. Hakuta, Nonlinear generation of 103 nm radiation with electromagnetically-induced transparency in atomic hydrogen. Quantum Opt. J. Eur. Opt. Soc. B **6**(4), 349–358 (1994)
49. V.G. Arkhipkin, Resonant Raman frequency mixing under electromagnetically induced transparency conditions. Quantum Electron. **27**(4), 341–345 (1997)
50. B.K. Clark, M. Masters, J. Huennekens, Wave mixing and amplified spontaneous emission in pure potassium and mixed sodium-potassium vapors. Appl. Phys. B Photophys. Laser Chem. **47**(2), 159–167 (1988)
51. Z.J. Jabbour, M.S. Malcuit, J. Huennekens, Broadly tunable near-infrared six-wave mixing processes in potassium vapor. Appl. Phys. B Photophys. Laser Chem. **52**(4), 281–289 (1991)
52. T. Efthimiopoulos, M.E. Movsessian, M. Katharakis, N. Merlemis, Cascade emission and four-wave mixing parametric processes in potassium. J. Appl. Phys. **80**(2), 639–643 (1996)
53. S.M. Hamadani, J.A.D Stockdale, R.N. Compton, M.S. Pindzola, Two-photon resonant four-wave mixing and multiphoton ionization of cesium in a heat-pipe oven. Phys. Rev. A **34**(3), 1938–1943 (1986)
54. M.A. Moore, W.R. Garrett, M.G. Payne, Suppression of electronic hyper-Raman emission by four-wave mixing interference. Opt. Commun. **68**(4), 310–316 (1988)
55. M. Malcuit, D. Gauthier, R. Boyd, W. York, Suppression of amplified spontaneous emission by the four-wave mixing process. Phys. Rev. Lett. **55**(10), 1086–1089 (1985)
56. W.R. Garrett, Forward gain suppression of optically pumped stimulated emissions due to self-induced wave-mixing interference during a pump pulse. Phys. Rev. Lett. **70**(26), 4059–4062 (1993)

57. M.E. Movsessian, A.V. Papoyan, S.V. Shmavonyan, Radiation amplification and image conversion in stimulated PFWM in potassium vapor. Int. J. Nonlinear Opt. Phys. **1**(4), 775–783 (1992)
58. N. Omenetto, O.I. Matveev, W. Resto, R. Badini, B.W. Smith, J.D. Winefordner, Nonlinear behaviour of atomic fluorescence in mercury vapours following double-resonance laser excitation. Appl. Phys. B Laser Opt. **58**(4), 303–307 (1994)
59. N. Merlemis, G. Papademetriou, D. Pentaris, T. Efthimiopoulos, V. Vaičaitis, Axial coherent emissions controlled by an internal coupling field in an open four-level potassium system. Appl. Phys. B **124**(7), 145 (2018)
60. D. Pentaris, T. Efthimiopoulos, N. Merlemis, A. Lyras, Control of the emission channels response in laser- potassium atom interaction. J. Phys. B: Atomic Mol. Opt. Phys. **205505**(45), 1–24 (2012)
61. H. Eicher, Third-order susceptibility of alkali metal vapors. IEEE J. Quantum Electron. **11**(4), 121–130 (1975)
62. D. Pentaris, D. Damianos, G. Papademetriou, A. Lyras, K. Steponkevičius, V. Vaičaitis, T. Efthimiopoulos, Coherently controlled emissions $|4P_{3/2,1/2}\rangle \leftrightarrow |4S_{1/2}\rangle$ from a femtosecond Λ-type excitation scheme in potassium atom. J. Mod. Opt. **0340**(February), 1–12 (2016)
63. M.O. Scully, S.M. Zubairy, *Quantum Optics*, 1st edn. (Cambridge University Press, London, 1997)
64. S.N. Dixit, P. Lambropoulos, Theory of photoelectron angular distributions in resonant multiphoton ionization. Phys. Rev. A **27**(2), 861–874 (1983)
65. S. Dixit, P. Lambropoulos, P. Zoller, Spin polarization of electrons in two-photon resonant three-photon ionization. Phys. Rev. A **24**(1), 318–325 (1981)
66. A.T. Georges, P. Lambropoulos, J.H. Marburger, Theory of third-harmonic generation in metal vapors under two-photon resonance conditions. Phys. Rev. A **15**(1), 300–307 (1977)
67. M.R. Teague, P. Lambropoulos, Three-photon ionization with spin-orbit coupling. J. Phys. B: Atomic Mol. Phys. **9**(8), 1251–1262 (1976)
68. A. Armyras, D. Pentaris, N. Merlemis, A. Lyras, T. Efthimiopoulos, The saturation effect of the parametric emission in potassium atoms under two-photon excitation. AIP Conf. Proc. **1288**, 80–83 (2010)
69. D. Pentaris, G. Papademetriou, T. Efthimiopoulos, N. Merlemis, A. Lyras, Emissions enhancement in a pump–coupling V-type coherently controlled four-level atomic system. J. Mod. Opt. **60**(21), 1855–1868 (2013)
70. G. Papademetriou, D. Pentaris, T. Efthimiopoulos, A. Lyras, Dynamic emission and population control in a Λ-type excitation scheme of atomic potassium. J. Phys. B: Atomic Mol. Opt. Phys. **50**(12), 125401 (2017)
71. E. Gaižauskas, D. Pentaris, T. Efthimiopoulos, V. Vaičaitis, Probing electronic coherences by combined two- and one-photon excitation in atomic vapors. Opt. Lett. **38**(2), 124–126 (2013)
72. B.W. Shore, *The Theory of Coherent Atomic Excitation*, vol. 1 (Wiley, New York, 1990)
73. C. Gardiner, P. Zoller, *Quantum Noise - A Handbook of Markovian and Non-Markovian Quantum Stochastic Methods with Applications to Quantum Optics* (Springer, Berlin Heidelberg, 2004)